Rotor Structure Selections of Nonsine Five-Phase Synchronous Reluctance Machines for Improved Torque Capability

Longya Xu, *Senior Member, IEEE*

***Abstract*—Five-phase synchronous reluctance machines (SynRM's) have a higher torque density over conventional three-phase SynRM's due to the utilization of the third harmonics in the magnetic field interacting with appropriate armature current. However, for effective utilization of the third harmonics, it is critical that the rotor of the SynRM creates sufficient coupling between the fundamental and third harmonic components in the field. This paper presents a comparison study of the rotor structures for the nonsine five-phase SynRM's with a detailed examination of two different reluctance rotor structures. The comparison results reveal that, with a simple structure, the salient-pole rotor creates strong mutual coupling between the fundamental and third harmonic MMF's and, thus, outperforms the complicated axially laminated rotor structures for nonsine five-phase SynRM's in terms of torque and ease of manufacturing.**

***Index Terms*—Axially laminated, five phase, nonsine, synchronous reluctance machine.**

I. Introduction

FOR the last ten years or so, interesting research work has been published on synchronous reluctance machines (SynRM's). It was noted that SynRM's with a higher number of phases (>3) have several advantages over a traditional three-phase SynRM. These advantages include a reduced current per phase for higher reliability, a reduced common-mode voltage for less EMI, and an increase of redundancy in the machine winding and associated converter device for fault tolerance [1]–[5]. In particular, for a five-phase SynRM, proper addition of the third harmonic to fundamental current can cause useful harmonic field-current interaction. As a result, a higher torque density ($>110\%$) can be accomplished in a five-phase nonsine than in a traditional three-phase sine-wave SynRM. It is, therefore, recognized that, in the five-phase SynRM, a magnetic field rich in fundamental and third harmonic components is the key to achieve high torque density.

In the previous research related to the SynRM, much attention has been directed to improving the rotor saliency ratio L_d/L_q, a critical parameter for accomplishing high torque density in sine-wave operation [3], [4]. In this regard, it was demonstrated that an axially laminated rotor is superior to the other rotor structures, except for the unfamiliarity and difficulty in manufacturing [5]. However, in terms of the nonsine-wave five-phase SynRM, the most suitable rotor remains undetermined. Nevertheless, it is pointed out that, if the harmonics are taken into account, the electromagnetic torque of the five-phase SynRM can be expressed as [2]

$$\begin{aligned} T_e = \frac{P}{2}\frac{5}{2}\{&[L_{md1} - L_{mq1}]i_{qs1}i_{ds1} \\ &+ 2L_{m13}[i_{qs3}i_{ds1} - i_{qs1}i_{ds3}] \\ &+ 3[L_{md3} - L_{mq3}]i_{qs3}i_{ds3}\}. \end{aligned} \tag{1}$$

Inspection of this equation immediately reveals that the first term in (1) is the torque component produced by fundamental current, much like that in a general three-phase sine SynRM. Also, the last term shows the contribution of the third harmonic current interacting with third harmonic field. Calculation shows that this term is very small and can be neglected. However, the most interesting term in (1) is the second one that indicates existence of mutual actions between the third harmonic current and the fundamental MMF to generate average torque. As will be proven later in this paper, this term can contribute 15% or more to the total torque production if a five-phase SynRM is properly designed and controlled.

From (1), it is also seen that if torque contribution of harmonics is considered as being obviously needed for the five-phase SynRM, the criterion of selecting a rotor design should be reexamined. That is, not only should the parameters associated with the fundamental field, such as L_{md1} and L_{mq1}, but also those characterizing the mutual coupling among the harmonic components, such as L_{m13}, be considered. From a practical point of view, needless to say, the ease and cost of manufacturing the rotor are important concerns.

Motivated by selecting a most suitable rotor structure for the five-phase SynRM with the third harmonics in operation, this paper studies two representative rotor structures in terms of torque production and ease of manufacturing. The investigation and evaluation starts with a concept discussion on mutual coupling between harmonic MMF's, and then is followed by a simplified linear model analysis of the two rotors. Next, a detailed nonlinear analysis is given using finite-element method (FEM) to deal with the complicated laminations and nonlinear magnetic materials. Finally, corresponding conclusions are obtained. The paper intends to reveal an important fact that the axially laminated rotor, although excellent in sine-wave

Paper IPCSD 00–008, presented at the 1999 Industry Applications Society Annual Meeting, Phoenix, AZ, October 3–7, and approved for publication in the IEEE TRANSACTIONS ON INDUSTRY APPLICATIONS by the Electric Machines Committee of the IEEE Industry Applications Society. Manuscript submitted for review June 15, 1999 and released for publication March 7, 2000.

The author is with the Department of Electrical Engineering, The Ohio State University, Columbus, OH 43210–1272 USA (e-mail: xu.12@osu.edu).

Publisher Item Identifier S 0093-9994(00)05423-2.

operation, does not match the five-phase SynRM harmonic operation in achieving high torque density, an issue that could be overlooked or be misleading due to its outstanding saliency ratio.

II. Harmonic MMF Interaction due to Reluctance Rotor

According to the traditional electric machine theory based on rotating field, it is fundamental that the stator and rotor poles will interact and produce average torque if and only if stator and rotor pole numbers are the same and their rotations are synchronized. Applying this theory to the nonsine five-phase SynRM with mixed stator MMF's, containing both fundamental and third harmonic components, the rotor should exhibit different pole numbers (for example, two and six) to match those of the stator MMF's. Otherwise, the SynRM contains no useful torque-producing mechanism. On the other hand, if the rotor does exhibit different pole numbers, the five-phase SynRM can be regarded as two seperate SynRM's built into a common frame with different pole numbers. In this way, the MMF's with different pole numbers are magnetically unrelated.

A. Concept of Harmonic MMF Mutual Coupling

A very important function that a reluctance rotor can play in the five-phase SynRM is to couple one MMF to another of different pole number, for example, interacting the two-pole MMF with the six-pole MMF, or vice versa [6], [7]. This is to say, when the stator is excited with fundamental current and produces a two-pole MMF, this two-pole MMF can be modulated by the rotor reluctance. As a result, a six-pole air-gap flux is produced and, if it rotates, the six-pole flux induces a third harmonic back EMF. Once the back EMF interacts with the third harmonic current, electromechanical energy conversion and average torque occur. This is the so-called mutual coupling between the fundamental and third harmonic MMF's, with the help of a reluctance rotor modulation. Since mutual coupling is reciprocal, analysis of mutual coupling can also start with the six-pole MMF under the reluctance rotor modulation to produce two-pole rotating field and then coupled to the fundamental MMF's.

The reluctance-rotor-created mutual coupling can be mathematically derived by the following example. Assume that, in the five-phase SynRM, both the fundamental and third harmonic MMF's are set up by the respective stator excitation. Then, a salient-pole rotor is placed into the stator frame with its inverse gap function described as

$$g^{-1} = \frac{G}{2}(1 + \cos 2(\phi - \theta_r)) \tag{2}$$

where G is a constant showing the mean of inverse air-gap size. ϕ denotes the air-gap angular position and θ_r the rotor displacement from the stator, respectively. Further, we assume that the rotor is synchronized with the MMF, that is, $\theta_r = \omega t$. Then, we can find the air-gap flux distribution due to the fundamental MMF $F_1 \sin(\omega t - \phi)$

$$\begin{aligned} B(\phi) &= g^{-1} \cdot F_1 \sin(\omega t - \phi) \\ &= \frac{G}{2} \cdot \frac{1}{2} F_1 [\sin(\omega t - \phi) + \sin 3(\omega t - \phi)]. \end{aligned} \tag{3}$$

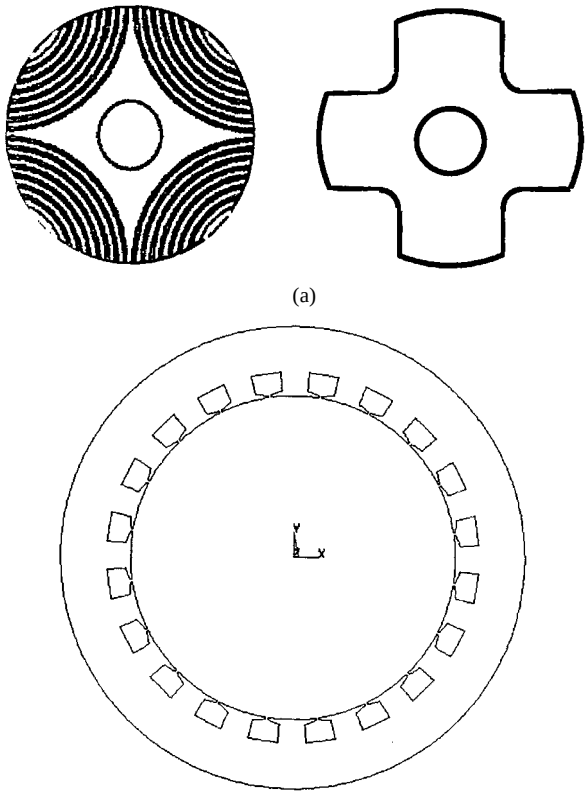

Fig. 1. (a) Salient-pole and axially laminated rotors. (b) Stator with concentrated windings.

Notice that the fundamental MMF has generated two air-gap fields, one with two poles and another with three times two poles. The latter is the third harmonic field produced by the modulation of the reluctance rotor. If interacting with the third harmonic current, average torque can be produced. Equivalently, with the induced third harmonic back EMF and injected current interacting with each other, electromagnetic energy conversion results. The striking feature of this particular torque or energy conversion is that it is achieved by two MMF's with different pole numbers, originated from two independent currents with different frequencies. It is apparent that the reluctance rotor here plays a key role in converting one pole number to another for the MMF's and, thus, creates mutual coupling between harmonics. Naturally, we will have a question as to how to characterize the degree of mutual coupling and how to select a rotor structure so that the obtained mutual coupling best meets the designer's expectation. We will discuss these interesting issues in this paper.

B. Two Types of Rotor Structures

The two rotor structures under examination are shown in Fig. 1(a) and both are to be placed into a common stator for comparison. The common five-phase SynRM stator is equipped with concentrated windings as shown in Fig. 1(b). The dimensions and stator winding specifications are summarized in Table I.

As shown in the Fig. 1(a), one rotor is a conventional salient pole type, regarded as poor in terms of salient ratio, and thus

TABLE I
DIMENSIONS AND WINDING SPECIFICATIONS

Rated Power	66 kw	Stator OD/ID	436.76 mm
Phase Number	5	Stator ID	305.46 mm
Rated Speed	1800 rpm	Core length	226.30mm
Rated Voltage	115 volts	Slot number	20
Rated Current	140 amps	Turn # per phase	14

achieves low torque production if only pure sine excitation is used. Nevertheless, the simple and rugged structure of this rotor has always been attractive for practical applications. The process of making such a salient-pole rotor is very easy and the cost is exceptionally low because of no rotor windings and permanent magnets.

The second rotor is of the axially laminated structure that has been under hot discussion by many researchers in recent years. Note that this rotor is constructed of axially laminated steel bent into a "u" or "v" shape and then stacked in the radial direction. The axially laminated rotor is considered superior to the other type of rotors in terms of saliency, but is very difficult and high in cost to manufacture [8], [9].

C. Stator Concentrated Windings and Resultant MMFs

The five-phase concentrated windings in the stator are in full pitch and each side of the winding occupies a single slot. The spatial displacement between the phases is one-fifth of a space cycle (electrical). Neglecting the high-order harmonics and expressed by winding functions, the five-phase concentrated windings are in the form of

$$\begin{aligned}
N_a &= \frac{4}{\pi}\frac{N}{2}\left[\cos p\phi - \frac{1}{3}\cos 3p\phi\right] \\
N_b &= \frac{4}{\pi}\frac{N}{2}\left[\cos\left(p\phi - \frac{2\pi}{5}\right) - \frac{1}{3}\cos 3\left(p\phi - \frac{2\pi}{5}\right)\right] \\
N_c &= \frac{4}{\pi}\frac{N}{2}\left[\cos\left(p\phi - \frac{4\pi}{5}\right) - \frac{1}{3}\cos 3\left(p\phi - \frac{4\pi}{5}\right)\right] \\
N_d &= \frac{4}{\pi}\frac{N}{2}\left[\cos\left(p\phi + \frac{4\pi}{5}\right) - \frac{1}{3}\cos 3\left(p\phi + \frac{4\pi}{5}\right)\right] \\
N_e &= \frac{4}{\pi}\frac{N}{2}\left[\cos\left(p\phi + \frac{2\pi}{5}\right) - \frac{1}{3}\cos 3\left(p\phi + \frac{2\pi}{5}\right)\right] \quad (4)
\end{aligned}$$

where N is the actual turns per pole per phase, and p is 2 for the four-pole SynRM under investigation. As represented by this set of equations, a concentrated winding is regarded approximately as a combination of two sinusoidally distributed windings, with different pole numbers and pole pitches. If the following set of five phase currents are sent to the stator windings, both fundamental and third harmonic MMF's are produced:

$$\begin{aligned}
i_a &= \sqrt{2}[I_1\sin\theta + I_3\sin 3\theta] \\
i_b &= \sqrt{2}\left[I_1\sin\left(\theta - \frac{2\pi}{5}\right) + I_3\sin 3\left(\theta - \frac{2\pi}{5}\right)\right] \\
i_c &= \sqrt{2}\left[I_1\sin\left(\theta - \frac{4\pi}{5}\right) + I_3\sin 3\left(\theta - \frac{4\pi}{5}\right)\right] \\
i_d &= \sqrt{2}\left[I_1\sin\left(\theta + \frac{4\pi}{5}\right) + I_3\sin 3\left(\theta + \frac{4\pi}{5}\right)\right] \\
i_e &= \sqrt{2}\left[I_1\sin\left(\theta + \frac{2\pi}{5}\right) + I_3\sin 3\left(\theta + \frac{2\pi}{5}\right)\right]. \quad (5)
\end{aligned}$$

Note that, in the five-phase current set, the amplitudes of the fundamental and third harmonic components are independently controllable with a power electronic converter. The phase difference between the neighboring phases in the set is one-fifth of a cycle in time. Considering the MMF created with the five-phase symmetric currents collectively, we can evaluate the production of winding function by current

$$\begin{aligned}
\mathrm{MMF}_{5\phi} = \sum_{n=1}^{5}\frac{4\sqrt{2}}{\pi}\frac{N}{2}\Bigg[&I_1\cos\left(p\phi - \frac{2(n-1)\pi}{5}\right) \\
&\times\sin\left(\theta - \frac{2(n-1)\pi}{5}\right) \\
&+\frac{1}{3}I_3\cos 3\left(p\phi - \frac{2(n-1)\pi}{5}\right) \\
&\times\sin 3\left(\theta - \frac{2(n-1)\pi}{5}\right)\Bigg]. \quad (6)
\end{aligned}$$

Facilitating the above equation, obviously, five-phase concentrated stator windings excited by the symmetric five-phase currents generate two synchronized sine rotating MMF components

$$\frac{5\sqrt{2}}{\pi}NI_1\cos(p\phi - \theta) \quad \text{and} \quad \frac{5\sqrt{2}}{3\pi}NI_3\cos 3(p\phi - \theta) \quad (7)$$

one in full pitch and another in one-third of full pitch. The two MMF's are rotating with the same speed in the airgap.

III. Linear Model Analysis of Rotor Structures

As indicated in (1), for a five-phase SynRM, the influential magnetizing inductance includes L_{md1}, L_{mq1}, L_{m13}, L_{md3}, and L_{mq3}. From a physics point of view, the first two parameters represent the SynRM capability of producing fundamental magnetic field (in space) along the d- and q-axes in the air gap, using fundamental current (in time). Similarly, the last two parameters represent the five-phase SynRM capability of producing the third harmonic field (in space) with a third harmonics sine-wave current (in time). As stated in many publications, the larger the difference between the d- and q-axes inductance parameters, the better the rotor structure, because torque production of the SynRM is maximized.

A. Significance of Mutual Inductance L_{m13}

Inductance L_{m13} is a unique parameter for the five-phase SynRM in that it represents the capability of producing third harmonic field by a fundamental current, or vice versa. If L_{m13} is large, it means that a large third harmonic field and, thus, a high third harmonic back EMF can be produced by the fundamental excitation. Equivalently, a large torque component can be produced by the interaction of the fundamental and the third harmonic currents. Therefore, the size of L_{m13} achievable determined by a reluctance rotor structure critically impacts the total torque production and performance of the five-phase SynRM.

The linear model for calculating mutual inductance with the salient-pole rotor is drawn in Fig. 2 with the stator winding functions. Notice that we have substituted the concentrated winding with a combination of fundamental and third harmonic windings. Further, we assume that the set of five-phase fundamental windings are excited with five-phase symmetric, fundamental currents. Therefore, a sine distributed MMF is established by

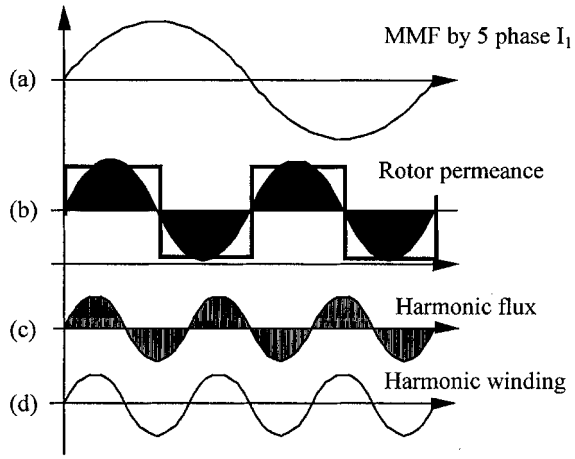

Fig. 2. Linear model of salient-pole rotor for L_{13} computation.

the five-phase fundamental current as shown in *(a)* of Fig. 2 that is synchronized with the reluctance rotor permeance shown in *(b)* of Fig. 2. With the rotor reluctance modulation taking into account, a third harmonic air-gap field will be generated in the wave shown in *(c)* of Fig 2. According to the winding function theory, it is easy to shown that the mutual inductance L_{m13} is the integration of the product of the two waves, *(c)* by *(d)* of Fig. 2, over the interval from 0 to 2π (see the Appendix). Without too much mathematical derivation, (6) gives the formula for computing L_{m13} by the simplified linear analysis, the same results as those obtained by a special d–q transformation in [2]

$$L_{m13} = \frac{10}{3} \cdot \frac{\mu_0 r l N^2}{\pi^2} \left(\frac{1}{g_a} - \frac{1}{g_b} \right) \tag{8}$$

where

- r stator inner radius;
- l effective length of stator;
- N turn number of winding per pole per phase;
- g_a minimum air gap along rotor pole area;
- g_b maximum airgap along rotor punched area.

Given the dimensions in Table I, the analytical results of L_{m13} for the salient-pole rotor is $L_{m13} = 0.98$ mH, one-sixth of $(L_{md1} - L_{mq1})$. It should be pointed out that, since mutual inductance follows reciprocal law, it is true that $L_{m13} = L_{m31}$. In the case of computing L_{31}, the excitation current will be given to the third harmonic windings and the air-gap flux from reluctance rotor modulation will be weighted by the fundamental winding.

B. Mutual Inductance With Axially Laminated Rotor

The axially laminated rotor is comprised of many layers of iron and insulators. This complicated rotor structure makes calculating mutual inductance L_{m13} extremely difficult by any analytical method. However, for simplicity without sacrificing essence, idealized characteristics of the axial laminations can be described, in that along the lamination direction, the rotor reluctance is zero and perpendicular to the lamination plane, infinite. Hence, all flux lines will flow along the lines defined by the laminations and the linear model for axially laminated rotor can be depicted in Fig. 3. According to this model, one lamination at location ϕ will form such a flux

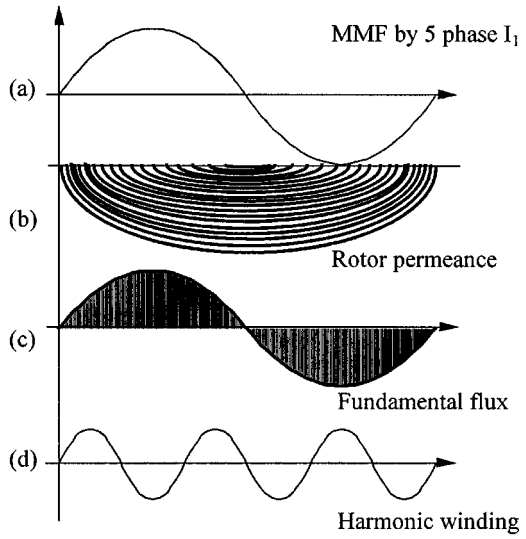

Fig. 3. Idealized flux paths set by axial laminations.

loop that the magnetic flux along the loop will be driven by $F_1[\sin\phi - \sin(\pi - \phi)] = 2F_1 \sin\phi$ and the reluctance is merely due to the constant air gap. Note that we have made a similar assumption for the stator winding functions as that in the case of salient-pole rotor analysis. However, the flux paths defined by the axial laminations are very different from those by the salient rotor. In the figure, special flux paths constrained by the axial laminations dislplay a particular air gap flux pattern as shown in *(c)* of Fig. 3. It can be observed that, for the fundamental MMF under the influence of the axially laminated rotor, the resultant air-gap flux distribution remains the same shape as that of the MMF. In other word, harmonic flux is not produced by the rotor reluctance modulation over the MMF. Applying (A-1) (see the Appendix) for integration to calculate inductance, the mutual inductance L_{m13} is identically zero because of being orthogonal between $B(\phi)$ and $N_3(\phi)$. More detailed analysis can show that, although the relative displacement between the MMF and the reluctance rotor will influence the magnitude, the basic shape of the air flux will not change. Therefore, it can be assured that the axially laminated rotor creates little mutual coupling between the fundamental and third harmonic MMF's.

IV. Nonlinear Analysis by FEM

To verify the preliminary results from linear analysis, the FEM is applied to consider nonlinearity of the core materials, complicated geometry of laminations and fringing effects. By two-dimensional (2-D) analysis, minor three–dimensional (3-D) end effects will be neglected. All dimensions of the five-phase SynRM in the finite-element analysis are kept the same as those used in linear models. Fig. 4 shows the discrete model of the SynRM in which only a quarter of the lamination is computed for the geometry quarter symmetry. Note that, to evaluate mutual coupling, the currents applied to the windings are assumed sine wave in time. The actual concentrated stator windings are realistically considered rather than being replaced by a combination of sinusoidal fundamental and third harmonic windings. For the salient-pole rotor, the ratio of pole arc to pole

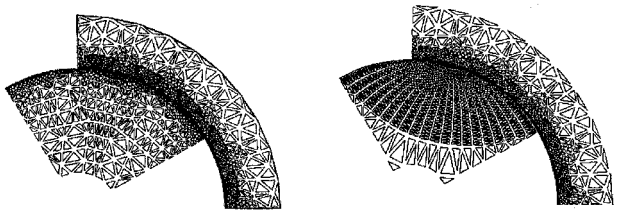

Fig. 4. Models of SynRM with two types of rotors in finite-element analysis.

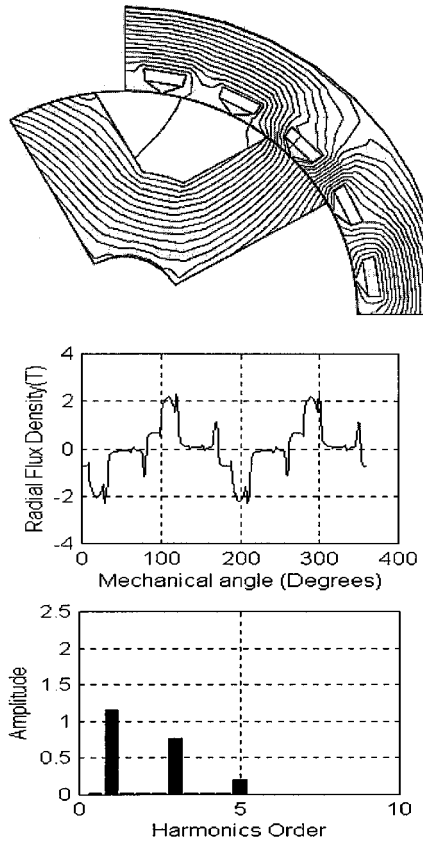

Fig. 5. Results of sine fundamental excitation with salient rotor.

pitch is 0.5 and for the axially laminated rotor, 0.7, in order to comply with manufacturability.

The computed area of the SynRM is divided into more than 4500 elements and the elements in the air gap are made very dense so as to ensure accuracy. Further, the rotor and stator are made separable and relative movement between the rotor and stator can be simulated in computation.

A. Flux Lines and Harmonic Contents

To verify the mutual coupling due to reluctance rotor modulation, it is critical to look at the air-gap flux distribution and its harmonic contents. For mutual coupling evaluation, the stator windings are excited with pure sine-wave currents that are maintained at a level to ensure core materials entering saturation. Then, the air-gap flux is plotted as a function of space angle and decomposed into Fourier series. The results for the case of the salient-pole rotor are shown in Fig. 5. From the top to bottom

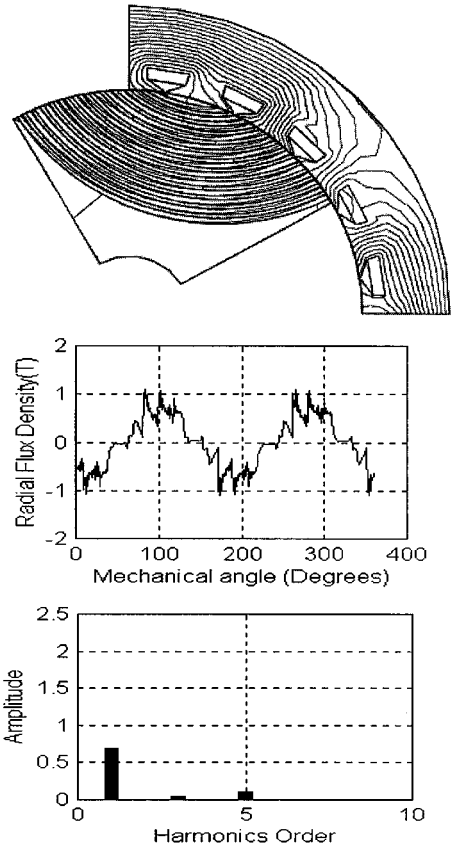

Fig. 6. Results of sine fundamental excitation with axially laminated rotor.

are the flux lines, distribution of the radial flux component, and harmonic contents of Fourier decomposition.

It is clearly seen from the results that a strong component of the third harmonic flux is created in the air gap by the fundamental excitation under the rotor reluctance modulation. Since this space harmonic flux has one-third of a full pitch, it can be linked and coupled easily to the third harmonic winding for back-EMF induction. Actually, the mutual inductance L_{13} is the integration over product of the normalized third harmonic flux by third harmonic winding function.

For the case of the axially laminated rotor, a similar computation is conducted and the results are shown in Fig. 6. In the computation, the only difference is that the salient-pole rotor is replaced by the axially laminated rotor. It can be easily observed from the results that the air-gap flux is very close to a sine distribution except for some slot effects. The third harmonic flux generated from the axially laminated rotor modulation is minimum, compared to that from the salient-pole rotor modulation. Although the third harmonic is not completely zero as compared to what was predicted by the linear model, the nonzero third harmonic component can be attributed to the fact that the axial lamination does not span a full pitch so that a minor nonsine modulation may take place. Because of the almost zero third harmonic component, the third harmonic winding hardly can link to any third harmonic flux originated from fundamental excitation. Therefore, the mutual coupling between the fundamental and third harmonic MMF's will be negligibly small.

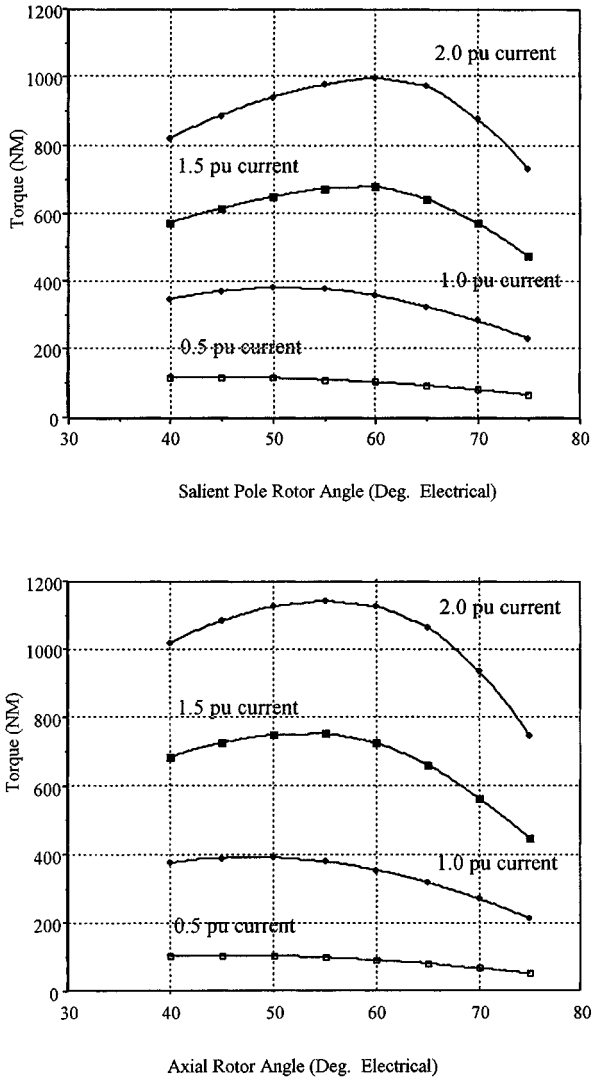

Fig. 7. Torque capability without third harmonic current.

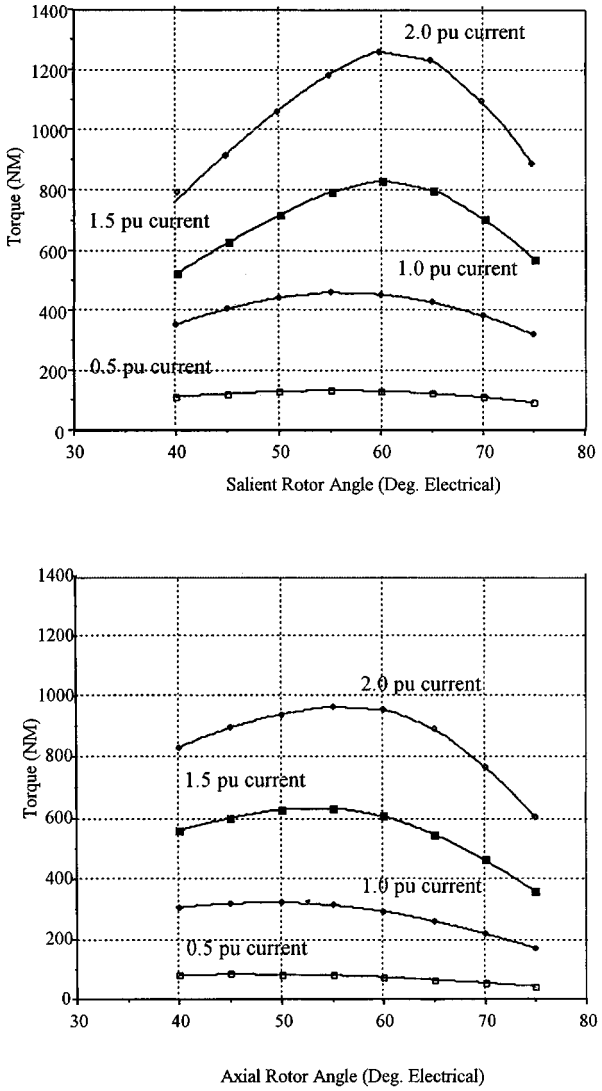

Fig. 8. Torque capability with third harmonic current (33%).

B. Comparison of Torque Capability

For both rotor structures, the torque performance is further investigated in detail by FEM to reveal effects of harmonic current. In the investigation, the stator currents are injected into the concentrated windings in two ways: one with pure sine waveforms and the other with an addition of 33% third harmonics to the fundamental. To have a fair comparison, the rms values of the currents are kept the same for sine and nonsine waveforms. Therefore, as the third harmonic current is added, the fundamental current is reduced proportionally so that copper losses remain identical in all cases. Another important factor for consideration is the rotor or torque angle versus the axis of the MMF. This is taken care of by varying the torque angle from 40° to 75° so that the peak torque generation for a given current level can always be displayed. Four current levels (0.5, 1.0, 1.5, and 2.0 p.u.) are selected for torque capability investigation.

The torque computation is based on magnetic field solution at different rotor angles and Maxwell tensor method is applied [10]. The results for both rotor structures without any harmonic current are shown in Fig. 7. As shown by the FEM results, for pure sine current operation, the SynRM with the axially laminated rotor clearly shows an advantage of higher torque capability. For this specific design of SynRM, at one p.u. current, about 5%, and two, nearly 18% more torque are produced by the axially laminated rotor than by the salient-pole SynRM's.

For the nonsine current operation with 33% being composed of the third harmonics, the torque capabilities of the SynRM are also calculated by FEM. The results are shown in Fig. 8, and the effect of the third harmonic current is quite evident. In the salient-pole rotor, the torque is boosted dramatically from 1000 without harmonic to 1250 N·m with harmonic for the same amount of rms value at the 2-p.u. level.

On the other hand, for the axially laminated rotor, when the 33% third harmonic current is put into stator windings, the torque capability is adversely reduced from 1150 to about 950 N·m. This is because, while the fundamental current is reduced, the added third harmonic current is almost useless for torque production. Therefore, the overall torque capability drops.

V. Conclusions

The following conclusions can be reached based on the work presented in this paper.

$$L_{m13} = \frac{1}{3}\frac{2N}{\pi}\frac{10N}{\pi^2}\left(\frac{1}{g_a} - \frac{1}{g_b}\right)\mu_0 rl \int_0^{2\pi} \sin(3\theta)\{\sin(\theta) - \sin(\theta)\cos(2\theta)\}\, d\theta. \tag{A-6}$$

1) For the five-phase nonsine SynRM with third harmonic in operation, not only should the parameters L_{md1} and L_{mq1} but also the mutual inductance L_{m13} be optimized to maximize torque density.
2) The salient-pole rotor, though, gives a relatively low salient ratio of L_{md1}/L_{mq1} but generates very strong mutual coupling between fundamental and third harmonics characterized by L_{m13}.
3) The axially laminated rotor has a high salient ratio but creates weak mutual coupling between the fundamental and third harmonics and, thus, it is not a good match for the five-phase nonsine SynRM.

It appears that, although the salient-pole rotor and five-phase SynRM stator match well for exploring advantages of the five-phase SynRM, the axially laminated rotor is still more suitable than the salient-pole rotor for pure sine-wave operation, except for the complicated manufacturing process and high cost. Taking robustness, cost, and ease of manufacturing into account, we consider that the salient-pole rotor is very competitive with the axially laminated rotor in the five-phase SynRM applications.

APPENDIX

According to the winding function theory, computation of the mutual inductance L_{m13} follows

$$\begin{aligned} L_{m13} &= \mu_0 rl \int_0^{2\pi} g^{-1}(\theta) F_{1-\bar{5}\phi}(\theta) N_3(\theta)\, d\theta \\ &= \mu_0 rl \int_0^{2\pi} B_{\bar{5}\phi}(\theta) N_3(\theta)\, d\theta \end{aligned} \tag{A-1}$$

where $g^{-1}(\theta)$ is the inverse gap function, $F_{1-\bar{5}\theta}(\theta)$ is the fundamental MMF generated by a set of five-phase symmetric currents with unity magnitude, and $N_3(\theta)$ is the winding function of the third harmonic winding

$$g^{-1}(\theta) = \frac{2}{\pi}(1 - \cos 2\theta)\left(\frac{1}{g_a} - \frac{1}{g_b}\right) \tag{A-2}$$

$$F_{1-\bar{5}\phi}(\theta) = \frac{5}{2}\frac{2N}{\pi}\sin\theta. \tag{A-3}$$

Interaction of the inverse air-gap function with the fundamental MMF generates the air-gap flux density as indicated by

$$\begin{aligned} B_{\bar{5}\phi}(\theta) &= g^{-1}(\theta) F_{1-\bar{5}\phi}(\theta) \\ &= \frac{2}{\pi}\frac{5}{2}\frac{2N}{\pi}\left(\frac{1}{g_a} - \frac{1}{g_b}\right)(1 - \cos 2\theta)\sin\theta \\ &= \frac{10N}{\pi^2}\left(\frac{1}{g_a} - \frac{1}{g_b}\right)(\sin\theta - \cos 2\theta \sin\theta). \end{aligned} \tag{A-4}$$

If the harmonic winding is in the form of

$$N_3(\theta) = \frac{1}{3}\frac{2N}{\pi}\sin(3\theta) \tag{A-5}$$

then, the mutual inductance will be evaluated by (A-6), shown at the top of the page. Note that, for the maximum nonzero results from integration, the variables inside the integration must be in-phase sine functions of the same frequency.

ACKNOWLEDGMENT

The author acknowledges and highly appreciates the assistance from B. Wang and W. Fu in computing numerous results by FEM.

REFERENCES

[1] H. A. Toliyat, L. Xu, and T. A. Lipo, "A five-phase reluctance motor with high specific torque," *IEEE Trans. Ind. Applicat.*, vol. 28, pp. 659–667, May/June 1992.
[2] H. A. Toliyat, S. P. Waikar, and T. A. Lipo, "Analysis and simulation of five-phase synchronous reluctance machines including third harmonic of airgap MMF," *IEEE Trans. Ind. Applicat.*, vol. 34, pp. 332–339, Mar./Apr. 1998.
[3] C. E. Coates, D. Platt, and B. S. P. Perera, "Design optimization of an axially laminated synchronous reluctance motor," in *Conf. Rec. IEEE-IAS Annu. Meeting*, Oct. 5–9, 1997, pp. 279–285.
[4] G. Oriti, A. L. Julian, and T. A. Lipo, "An inverter/motor drive with common mode voltage elimination," in *Conf. Rec. IEEE-IAS Annu. Meeting*, Oct. 5–9, 1997, pp. 587–592.
[5] J. S. Hsu, S.-S. P. Liou, and H. H. Woodson, "Peaked-MMF smooth-torque reluctance motors," *IEEE Trans. Energy Conversion*, vol. 5, pp. 104–109, Mar. 1990.
[6] L. Xu, F. Liang, and T. A. Lipo, "Transient model of a doubly excited reluctance motor," *IEEE Trans. Energy Conversion*, vol. 6, pp. 126–133, Mar. 1991.
[7] Y. Liao and C. Sun, "A low cost, robust position sensorless control scheme for DFRM drives," in *Cpnf. Rec. IEEE-IAS Annu. Meeting*, Toronto, ON, Canada, 1993, pp. 437–444.
[8] W. L. Soong, D. A. Staton, and T. J. Miller, "Design of a new axially laminated PM motor," in *Conf. Rec. IEEE-IAS Annu. Meeting*, Toronto, ON, Canada, 1993, pp. 27–36.
[9] A. Fratta, G. Trpglia, A. Vagati, and F. Villata, "Evaluation of torque ripple in high performance synchronous reluctance machines," in *Conf. Rec. IEEE-IAS Annu. Meeting*, Toronto, ON, Canada, 1993, pp. 163–170.
[10] *FEM Application Manual, ANSYS5.0*, Swanson Analysis Systems, Inc., Houston, PA, 1993.

Longya Xu (S'89–M'90–SM'93) received the M.S. and Ph.D. degrees from the University of Wisconsin, Madison, in 1986 and 1990, respectively, both in electrical engineering.

He has served as a Consultant to several companies, including Raytheon Company, U.S. Wind Power Company, General Motors, Ford, and Unique Mobility Inc. In 1990, he joined the Department of Electrical Engineering, The Ohio State University, Columbus, where he is currently an Associate Professor. His research and teaching interests include dynamic modeling and optimized design of electrical machines and power converters for variable-speed generating and drive systems, and application of advanced control theory and digital signal processors in controlling motion systems for super-high-speed operation.

Dr. Xu currently serves as the Chairman of the Electric Machines Committee of the IEEE Industry Applications Society (IAS) and as an Associate Editor of the IEEE TRANSACTIONS ON POWER ELECTRONICS. He received the 1990 First Prize Paper Award from the Industrial Drives Committee of the IAS. In 1991, he was the recipient of a Research Initiation Award from the National Science Foundation. He was also the recipient of Lumley Research Awards in 1995 and 1999 for his research accomplishments from the College of Engineering, The Ohio State University.